Protective effect of *Moringa oleifera* Lam. leaf extract against oxidative stress, inflammation, depression, and apoptosis in a mouse model of hepatic encephalopathy

Mohammed S. Mahmoud (msm07@fayoum.edu.eg)
Fayoum University Faculty of Science https://orcid.org/0000-0002-9190-6590
Attalla F. El-kott
Department of Biology College of Science, King Khalid University
Hussah I.M. AlGwaiz
Department of Zoology, College of Science, Princess Nourah bint Abdulrahman University
Samah M. Fathy
Faculty of Science, Fayoum University https://orcid.org/0000-0002-7870-7626

Research Article

Keywords: Behavioral changes, Hepatic encephalopathy, Inflammation, Moringa oleifera Lam., Neuroprotection, TLR4/2-MYD88/NF-κB pathway

Posted Date: April 6th, 2022

DOI: https://doi.org/10.21203/rs.3.rs-346191/v2

Version of Record: A version of this preprint was published at Environmental Science and Pollution Research on June 30th, 2022. See the published version at https://doi.org/10.1007/s11356-022-21453-x.

Abstract

The present study aimed to assess the antioxidative, anti-inflammatory, antiapoptotic, and anti-depression impacts of *Moringa oleifera* Lam. leaf ethanolic extract (MOLE) in the hippocampus and cerebral cortex of CCl_4-induced mouse model of hepatic encephalopathy. High-performance liquid chromatography was used to detect marker compounds; rutin and β-sitosterol. Animals were divided into four groups; vehicle group, CCl_4 treated group, MOLE treated group, and (CCl_4+ MOLE) group treated with MOLE for 14 days before CCl_4-induced neurotoxicity. MOLE decreased alanine aminotransferase, aspartate aminotransferase, corticosterone, and ammonia levels in serum and improved the antioxidant status of CCl_4 treated mice in the hippocampus and cerebral cortex. It reduced the expression of toll-like receptor (TLR)4, TLR2, myeloid differentiation primary response 88 (MYD88), and nuclear factor-kappa B (NF-κB) genes and the protein levels of the pro-inflammatory cytokines. MOLE also attenuated apoptosis, as revealed by the reduced expression of caspase3, and prevented histological deterioration. Furthermore, MOLE attenuated CCl_4-induced anxiety and depression-like behavioral changes. Collectively, MOLE modulates neuroinflammation, oxidative stress, TLR4/2-MyD88/NF-κB signaling, and apoptosis in the hippocampus and cerebral cortex of the hepatic encephalopathy experimental model.

Introduction

Chlorinated volatile compounds (Cl-VOC) have been reported to affect several organs such as the liver, the kidney, the heart, and the central nervous system (Genc et al. 2012; Teschke 2018; Webb et al. 2018). Furthermore, direct exposure to Cl-VOCs can cause oesophageal cancer, cervical cancer, and liver cancer (Lang and Beier 2018). For these devastating effects, some of them including Carbon tetrachloride (CCl_4) and chloroform (CHCl3) were considered priority pollutants by the United States Environmental Protection Agency (EPA) (Halawy et al. 2022). the γ-Al2O3 nanocomposite was suggested in a recent study as a cost-effective method to adsorb and remove CCl_4 (Halawy et al. 2022).

According to their review of hepatic encephalopathy animal models, the International Society of Hepatic Encephalopathy and Nitrogen Metabolism (ISHEN), CCL_4 can be used to induce hepatic encephalopathy (HE) in rodents by disrupting the hepatocytes leading to hyperammonemia, which subsequently results in neuroinflammation and decrease in neurogenesis and memory accusation (DeMorrow et al. 2021). CCl_4 is a neurotoxic substance used to mimic brain manifestations of people suffering from acute or chronic hepatic damage by triggering lipid peroxidation and alterations in the antioxidative mechanisms in the brain (Vairappan, Sundhar, and Srinivas 2019). The symptoms in patients include cognitive decline, motor, psychiatric disorders, and HE (Vairappan, Sundhar, and Srinivas 2019). HE is a neuropsychiatric disorder propagated as a result of acute or chronic hepatic failure (El-Marasy, El Awdan, and Abd-Elsalam 2019).

In the liver, CCl_4 is metabolized into highly reactive free radicals which oxidize fatty acids in the phospholipids of cell membranes leading to structural and functional changes in these membranes (Yue

et al. 2020). Moreover, these free radicals and CCl_4 cause injuries in the endoplasmic reticulum with a consequential effect on protein synthesis leading to lipid accumulation (Yue et al. 2020). Meanwhile, CCl_4 leads to producing inflammatory mediators from the triggered macrophages in the liver with accompanying systemic inflammation exerting a critical role in aggravating neurological manifestations, possibly by activating the predisposition of the brain to the associated hyperammonemia (Aldridge, Tranah, and Shawcross 2015).

Neuroinflammation and oxidative stress are involved in depression and anxiety development (Mello et al. 2013). Noteworthy, CCl_4 induces neuropsychiatric disorders mimicking what appears in patients with acute or chronic liver damage by targeting the brain antioxidative system and inflammatory pathways such as the toll-like receptor (TLR)4/nuclear factor-kappa B (NF-κB) pathway (Shal et al. 2020). Moreover, it has been reported that corticotropin-releasing factor (CRF) hypersecretion in response to the release of proinflammatory cytokines is attributable to modifying the hypothalamic-pituitary-adrenal (HPA)-axis resulting in increased plasma corticosterone levels and exacerbation of depression symptoms (Furtado and Katzman 2015).

Plants are well known for having therapeutic effects and have been used in traditional and modern medications. *Moringa oleifera* Lam. (MOL), family Moringaceae (Fakurazi, Sharifudin, and Arulselvan 2012) is widely known as the “Miracle Tree” due to its medicinal outcomes. Leaves, the most common and suitable part of the plant for medicinal commercial mass production (Mahdi et al. 2018) can be consumed in different ways then dried and stored for months without losing nutritional benefits (Tesfay et al. 2011). Our previous study recorded the following compounds in *Moringa oleifera* Lam. leaf ethanolic extract (MOLE); quercetagetin-7-O-glucoside, quercetin 3,5,7,3',4'-pentamethyl ether, and β-sitosterol along with other phytochemicals using gas chromatography-mass spectrometry (GC-MS) analysis (Fathy and Mahmoud 2021). Moreover, the total phenolic and the total flavonoid contents in MOLE were also measured (Fathy and Mahmoud 2021). Furthermore, MOL possesses pain relief, antidepression, antiinflammatory, immunomodulatory, and neuroprotective activities (Kou et al. 2018).

The current study aimed to assess the antioxidative, anti-inflammatory, antiapoptotic, and anti-depression impacts of MOLE in the HC and CC of CCl_4-induced HE mouse model. The alleviation potentials of MOLE were assessed by tracking its effect on the TLR4/2-MyD88/NF-κB pathway, neuroinflammation, apoptosis, oxidative stress, anxiety and depression-like behavior, and histopathological changes in the hippocampus (HC) and cerebral cortex (CC) regions of the mouse brain.

Materials And Methods

Chemicals

CCl_4 was purchased from Sigma (St. Louis, MO, US). All other chemicals and reagents used were of the highest analytical grade.

MOL source and identification

The source for the plant leaves was from Jazan city, KSA with latitude: 16° 53' 12.59" N and longitude: 42° 33' 23.99" E coordinates according to degrees minutes seconds (DMS). The authentication of the plant was carried out by taking the herbarium specimens found at Jazan University Herbarium (JAZUH), KSA, as a reference.

Preparation of MOLE

MOL leaves were washed, dried, and finally ground. 96% ethanol was mixed with the ground leaves and the mixture was kept in the shaking incubator at 37°C for 24 h. The obtained extract was then filtered and put in the rotary evaporator at 40°C until the ethanol was completely evaporated. Finally, a semi-solid extract was produced and stored at 4°C until use.

High-performance liquid chromatography (HPLC) analysis

MOLE was analyzed using the HPLC method for a qualitative analysis of two marker compounds. About 50 mg of the extract were dissolved in 25 mL methanol and injected into an HPLC (Agilent 1200 series, UV detector). For rutin, Agilent Eclipse XDB-C18 (150 × 4.6 mm, 5 µm), wavelength 254 nm, and 1 mL/min flow rate. The mobile phase consisted of acetonitrile: water/0.1 formic acid with a gradient increased from 5% to 95% over 15 min. For β-sitosterol, a waters symmetry shield C18 column (150 × 4.6, 5 µm) and wavelength 210 nm was used. The mobile phase consisted of methanol: acetonitrile with a ratio of 30:70 (v/v), with 1.0 mL/min flow rate.

Experimental design

Adult healthy BALB/c male albino mice weighing 20 - 25 g (8 weeks old) were brought from the National Cancer Institute (NCI). Throughout the experiment, animals were kept in conventional cages at the standard temperature, humidity, and light/dark cycle conditions. Animals had free access to the standard food and drink *ad libitum*.

The experiment lasted 15 days following a week of acclimatization. Animals were randomly divided into four groups with eight mice in each group; vehicle group (group 1), CCl_4-treated group (group 2), MOLE-treated group (group 3), and CCl_4+MOLE-treated group (group 4). The first two groups received distilled water orally by gavage daily for consecutive 14 days. The last two groups received MOLE (400 mg/kg body weight) (Singh et al. 2014) orally by gavage daily for consecutive 14 days. On day 15, group 2 and group 4 were then given a single dose of CCl_4 (1 mL/kg body weight) prepared by dilution in olive oil; 1:1 (v/v), intraperitoneally (*i.p.*) (Makni et al. 2012; Shal et al. 2020), while other groups (groups 1 & 3) received olive oil, (*i.p).* Behavioral tests were carried out in separate animal groups 24 hours later (Shal et al. 2020). For quantitative reverse transcription-polymerase chain reaction (RT-qPCR), the enzyme-linked immunosorbent assay (ELISA), and the evaluation of biochemical parameters, the animals were euthanized by decapitation under *i.p.* injection with pentobarbital (30 mg/kg) anesthesia.

Estimation of depression-like behavior by forced swimming test (FST) and tail suspension test (TST)

FST was carried out as described by Porsolt, Bertin, and Jalfre (1977). Initially, each mouse was placed inside a transparent cylinder in the water at a depth of 20 cm and a temperature of 23°C ± 2°C. Afterwards, the mice were individually forced to swim for 6 min. The time of immobility was recorded by considering the halt of escape-oriented behavior during the last 5 min.

TST was also executed as reported by Steru et al. (1985). For 6 min, each mouse was hung about 1 cm from the tip of its tail with adhesive tape on the edge of a rod at a height of 50 cm above the floor. The duration of immobility time was considered by recording the time each mouse was suspended without any activity or any motion in the last 5 min.

Collection of blood and tissue samples

The blood was collected and the serum was isolated by centrifugation at 2000 × g for 15 min at 4°C for biochemical analysis.

Brains were dissected from the skull. For the histopathological investigation, one side of each brain was kept in 10% neutral buffered formalin for later use. HC and CC were excised from the other side and assigned into two portions. The first portion of each region was homogenized in 1.5% KCl, centrifuged at 5000 × g, and the protein concentration in the tissue supernatant was evaluated following the Bradford method using the Biorad assay kit (Bradford 1976). The analysis of oxidative stress parameters and proinflammatory cytokines in the supernatant was followed. The second part from each brain region was collected in RNA lysis buffer to measure the gene expression of the inflammatory and apoptotic mediators.

Histopathological examination

After washing the tissue samples, a series of diluted alcohol was used for dehydration, followed by clearance in xylene, infiltration in paraffin wax, and embedding in paraffin wax blocks. For the histopathological examination, 5 µm thickness coronal sections were obtained and stained with Ehrlich's hematoxylin and eosin (H&E) as demonstrated by Bancroft and Gamble (2008). The thickness of dentate gyrus (DG) in HC was measured in different groups using ImageJ software.

RT-qPCR assay

Total RNA was isolated from the HC and CC tissues using SV Total RNA Isolation System (Promega Corporation, Madison, WI, US) as previously described (Fathy and Said 2019). RNA concentration and purity were analysed using the NanoDrop™ 2000/2000c Spectrophotometer (ThermoScientific, Lo, UK). Complementary DNA (cDNA) was then prepared using SuperScript III First-Strand Synthesis System following the manufacturer's instructions (Fermentas, Waltham, MA, US). The cDNA yield was then used to detect the relative expression levels of *TLR2*, *TLR4*, myeloid differentiation primary response 88 (*MYD88*), *caspase 3*, and *NF-κB* genes. Glyceraldehyde 3-phosphate dehydrogenase (*GAPDH*)

housekeeping gene was used for data normalization. Table 1 shows the primer sequences of mice genes used in the present study.

Determination of proinflammatory cytokines in HC and CC

The protein level of tumor necrosis factor (TNF)-α and interleukin (IL)-6 was detected in HC and CC supernatant by ELISA kits particularly for mice (Merck Millipore, San Francisco, California, US) following the producer's protocol. Protein levels were measured using the microplate ELISA reader at 450 nm.

Evaluation of biochemical parameters

Alanine aminotransferase (ALT) and aspartate aminotransferase (AST) levels in serum

Liver functions were determined by measuring ALT as described by Hafkenscheid and Dijt (1979) and AST according to Sampson et al. (1980) in serum using the enzymatic methods.

Detection of ammonia level in serum

Ammonia assay was used to assess the level of ammonia in serum, as described by Gutiérrez-de-Juan et al. (2017). The reaction of Nessler's reagent is the key to detecting ammonia production using ammonium chloride as a standard. The spectrophotometer was used at 425 nm, and the results were presented in percentages.

Evaluation of corticosterone level in serum

Serum corticosterone concentration was determined in serum by using ELISA kits (ThermoScientific, Lo, UK) as per the manufacturer's instructions. The levels were measured using the microplate ELISA reader at 450 nm.

Determination of malondialdehyde (MDA) level in the HC and CC

The lipid peroxidation (LPO) was measured in the homogenates' supernatant of each brain region based on thiobarbituric acid (TBA) reaction with MDA (Ohkawa, Ohishi, and Yagi 1979). The principle for the reaction is the formation of a product due to the LPO of the membranes. After incubation, the spectrophotometer was used to record the absorbance at 532 nm (MDA Colorimetric/Fluorometric Assay kit, Biovision Inc., CA, US).

Enzymatic and non-enzymatic antioxidants' levels in HC and CC

OxiSelect Superoxide dismutase (SOD) kit (CellBiolabs, Inc., CA, US) was used for detecting the activity of SOD as described by the producer's protocol following the method reported by Valentine and Hart (2003). The absorbance was recorded spectrophotometrically at 540 nm.

Reduced glutathione (GSH) level was measured using the method modified by Jollow et al. (1974). The basis for the assay depends on the formation of a yellow color due to the reaction between 5, 5-dithiobis-

2 nitro benzoic acid (DTNB) and free thiol groups of GSH. The absorbance was determined spectrophotometrically at 412 nm.

Statistical methods

Statistical analyses were performed using GraphPad PRISM (version 8.4.3 (686); Graph Pad Software, US). Data were represented as mean ± SD. Analyses were done using one-way analysis of variance (ANOVA) followed by Tukey's multiple comparison test. Differences were considered significant at $P < 0.05$. *: $P < 0.05$, **: $P < 0.01$, ***: $P < 0.001$, and ****: $P < 0.0001$ compared to vehicle group. #: $P < 0.05$, ##: $P < 0.01$, ###: $P < 0.001$, and ####: $P < 0.0001$ compared to CCl_4 group.

Results

Rutin and β-sitosterol detection by HPLC

For HPLC analysis, the authentic reference standards of rutin and β-sitosterol were analyzed using an identical chromatographic method. By comparing the peak retention times, rutin and β-sitosterol were identified in MOLE (Fig. 1).

MOLE pretreatment reverses the increase in serum aminotransferases, ammonia, and corticosterone levels induced by CCl_4

CCl_4 treatment for 24 hours remarkably increased ALT ($P < 0.01$) and AST ($P < 0.001$). These increases were markedly prevented in response to MOLE pretreatment at significances of ($P < 0.01$) and ($P < 0.001$) for ALT and AST, respectively (Fig. 2 a, b).

An apparent increase in serum ammonia levels was manifested in CCl_4-treated mice ($P < 0.0001$). However, MOLE pretreatment remarkably reversed this change ($P < 0.0001$), Fig. 2 (c).

Serum corticosterone levels were measured to investigate the potential role of MOLE against the alteration in the HPA-axis induced by CCl_4 treatment. A significant increase in serum corticosterone level was found in CCl_4-treated mice ($P < 0.01$). However, this increase was markedly prevented upon MOLE pretreatment ($P < 0.01$), Fig. 2 (d).

MOLE pretreatment alleviates oxidative stress induced by CCl_4

The role of MOLE pretreatment against CCl_4 LPO was investigated by measuring MDA in the HC and CC brain tissues. CCl_4 significantly increased LPO in both HC and CC as evidenced by the striking increase in MDA ($P < 0.0001$). This effect was remarkably attenuated in both tissues in the presence of MOLE pretreatment ($P < 0.001$), Fig. 3 (a, b).

SOD and GSH levels were measured in the HC and CC brain tissues to evaluate the potential antioxidant power of MOLE against CCl_4 neurotoxicity. CCl_4 markedly enhanced the oxidative stress as evidenced by

the significant decrease in SOD and GSH levels in the HC ($P < 0.05$) and CC ($P < 0.01$). However, MOLE administration before CCl_4 treatment attenuated these decreases significantly in both tissues ($P < 0.05$), Fig. 3 (c-f).

The effect of MOLE pretreatment against inflammatory response initiated by CCl_4

MOLE pretreatment effect on TLR4/2-MyD88/NF-κB pathway

RT-qPCR was used to measure the expression of *TLR2*, *TLR4*, *MyD88*, and *NF-κB* genes in the HC and CC brain tissues to evaluate the role of MOLE pretreatment on the TLR4/2-MyD88/NF-κB pathway. CCl_4 significantly increased the gene expression of *TLR2* ($P < 0.001$), *TLR4* ($P < 0.001$) and *MyD88* ($P < 0.0001$) in both brain regions. *NF-κB* gene expression was also significantly upregulated in response to CCl_4 toxicity in the HC ($P < 0.01$) and CC ($P < 0.05$). Most of these increases were significantly alleviated in response to MOLE pretreatment. *TLR2* gene expression was significantly reduced in both HC ($P < 0.01$) and CC ($P < 0.001$). *TLR4* gene expression was also significantly decreased in both tissues ($P < 0.001$). A marked restoration of *MyD88* gene expression was also noted ($P < 0.0001$). Although a decrease in *NF-κB* gene expression was noted in both tissues, it was only significant in the HC ($P < 0.01$), (Table 2).

MOLE pretreatment reverses alterations in TNF-α and IL-6 levels induced by CCl_4

The effect of MOLE pretreatment on the inflammatory mediators activated by CCl_4 was evaluated by measuring TNF-α and IL-6 protein levels in the HC and CC brain tissues in different groups. CCl_4 significantly increased the protein levels of TNF-α and IL-6 in both HC and CC ($P < 0.01$). Nevertheless, pretreatment with MOLE remarkably prevented these elevations in the HC ($P < 0.05$) and CC ($P < 0.01$), (Table 2).

MOLE exhibits an antiapoptotic effect against CCl_4 neurotoxicity

Caspase 3 gene expression was measured in the HC and CC brain tissues to assess the antiapoptotic effect of MOLE against CCl_4 neurotoxicity. A remarkable increase in *caspase 3* gene expression was manifested in both brain tissues in response to CCl_4 toxicity ($P < 0.0001$). However, MOLE was found to have an antiapoptotic role against this effect as evidenced by the striking decrease in *caspase 3* gene expression in both tissues ($P < 0.0001$), (Table 2).

MOLE protects against depression-like behavior induced by CCl_4

FST and TST were performed to investigate the protective role of MOLE pretreatment against depression-like behavior manifested in CCl_4-treated mice. Depression-like behavior was represented by mice immobility in seconds after FST and TST were recorded. CCl_4 was found to significantly increase depression-like behavior based on both FST ($P < 0.01$) and TST ($P < 0.0001$). Nevertheless, pretreatment with MOLE had a marked anxiolytic effect as evidenced by FST ($P < 0.01$) and TST ($P < 0.001$), (Fig. 4).

MOLE pretreatment protects against histopathological changes induced in brain regions by CCl_4

Coronal sections in the HC and CC were stained with H&E to assess the neuroprotective effect of MOLE against histopathological alterations induced by CCl_4. CCl_4 induced histopathological changes including thinning of the DG region in the HC (Fig. 5) and neuron degeneration in the CC (Fig. 6). However, MOLE pretreatment significantly alleviates these changes.

Discussion

HE is ascribed with hyperammonemia in the bloodstream that can pass via the blood-brain barrier (BBB) and causes damage to the brain tissue through oxidative stress, inflammatory response, and dysfunction of energy metabolism (de Souza Machado et al. 2015) . It is well known that CCl_4 treatment can successfully stimulate liver injury and HE associated brain tissue damage (de Souza Machado et al. 2015) . For confirmation, the current experiment revealed that serum levels of liver enzymes; ALT and AST were increased significantly in CCl_4-induced mice compared to the vehicle group. Pretreatment with MOLE halts the increase of ALT and AST levels in CCl_4-treated mice.

In the present study, CCl_4 induced oxidative stress whereas MOLE pretreatment protected brain tissue from oxidative stress damage. In the current study, an increase in MDA and a decrease in antioxidants were observed in HC and CC following CCl4 injection. CYP450-mediated bioactivation of CCl_4 into reactive free radicals; trichloromethyl (CCl_3), and trichloromethyl peroxy radical (CCl_3OO) initiates hepatocyte damage. This initiation activates the release of reactive oxygen species (ROS) leading to LPO (Risal et al. 2012) . The severity of LPO from cell membranes can be monitored by assessing the MDA formed in brain tissue (Lıu and Tıan 2016) . Moreover, the decline in GSH and SOD levels was reportedly due to ROS release in the CCl_4 mouse model of encephalopathy (Ogaly, Eltablawy, and Abd-Elsalam 2018) . The dysregulated antioxidant mechanism in the current model was consistent with previous reports (Han et al. 2019; Shal et al. 2020) , where an elevated MDA and reduced antioxidant mechanism in different brain regions were observed after CCl_4 intoxication. MOLE pretreatment successfully restored the antioxidative power in HC and CC by reducing MDA and restoring antioxidative mechanisms, consistent with Idoga et al. (2018) . The reversed alterations of antioxidant power in MOLE/CCl_4 treated mice demonstrate the neuroprotective effect of MOLE and its prominent antioxidant capacity protecting against LPO.

It was recorded that Inflammation is a crucial inducer of HE (Lu et al. 2020) . Liver damage was associated with peripheral inflammation and cytokine storming that can cross BBB with ascribed neuroinflammation disorders (Lu et al. 2020) . To evaluate the protective effects of MOLE against neuroinflammation consequences in HC and CC regions of CCl_4 injected mice, relative expressions of *TLR2*, *TLR4*, *MyD88*, and *NF-κB* genes as well as the protein levels of TNF-α and IL-6 were measured.

Toll-like receptors (TLRs) play major roles in inflammatory responses (Kong and Le 2011) . TLR2 and TLR4 are considered neuroinflammatory receptors residential in neurons, astrocytes, and microglia (Mao et al. 2012) . Almost all TLRs adaptor protein is MyD88. It links the receptors and the downstream signaling components with subsequent activation of transcription and inflammatory responses (Mao et al. 2012) . The current experiment detected upregulation of *TLR4*, *TLR2*, and *MyD88* gene expressions in CCl_4 treated mice. Our findings were consistent with previous studies (Lu et al. 2020; Zhou et al. 2020) where upregulated *TLR4*, *TLR2*, and *MyD88* gene expressions were noticed in HE rat model. MOLE interferes with this cascade as evidenced by the downregulation of *TLR4*, *TLR2*, and *MyD88* gene expressions manifested in the CCl_4/MOLE-treated group.

Gene expression of *NF-κB* was also elevated in the present CCl_4 treated mice and was downregulated by MOLE pretreatment. In addition, activating the TLR4/2-MyD88 dependent signaling pathway has been reported to lead to *NF-κB* transcription (Zhou et al. 2020) . Consequently, the TLR4/2-MyD88/NF-κB signaling pathway might be targeted by MOLE to mitigate CCl_4 toxicity.

TLR4, a member of TLRs, has been evidenced to play a significant role in initiating the inflammatory response after brain damage (Brown et al. 2011) . The present study found an increase in proinflammatory cytokines in the CCl_4 group, prevented in the CCL_4 + MOLE group. CCl_4 toxicity increases the levels of proinflammatory cytokines produced by Kupffer cells. Consequently, liver stromal cells are recruited to assist in intensifying the inflammatory response by producing cytokines and chemokines (Shim et al. 2010) . This peripheral intensification in inflammatory response activates microglia and TLR4. Microglial activation is ascribed to the secretion of proinflammatory cytokines such as IL-6 and TNF-α that were associated with the brain deteriorations observed in CCl_4 treated mice (Vairappan, Sundhar, and Srinivas 2019) . Whereas TLR4 activation exacerbates the inflammatory reactions by inducing the NF-κB pathway leading to the generation of proinflammatory factors (Yoshimura and Shichita 2012) .

Oxidative stress and neuroinflammation are associated with neurobehavioral changes (Kubera et al. 2011) . For instance, proinflammatory cytokines such as IL-1β, IL-6, and TNF-α are increased in depression and anxiety, implying immune dysregulation (Dowlati et al. 2010) . Moreover, symptoms of depression were proven to be aggravated by proinflammatory cytokines, leading to disturbance of the HPA-axis as a result of hypersecretion of CRF with elevated corticosterone level in plasma and subsequent induction of depression symptoms (Furtado and Katzman 2015; Shal et al. 2020) . Subsequently, the neuroprotective effect of MOLE against CCl_4-induced anxiety and depression-like behavioral changes via FST and TST was assessed. CCl_4-induced anxiety and depression-like behavioral changes observed in the current study agree with a previous report (Shal et al. 2020) . However, pretreatment with MOLE significantly improved the mice's behavioral status. This improvement may indicate that MOLE contains anxiolytic and antidepression phytochemicals. These phytochemicals could act on serotonergic, dopaminergic, and/or noradrenergic neurotransmitter systems (Millan 2004) .

Besides, the elevated corticosterone level in CCl_4-treated mice was alleviated by MOLE pretreatment in the current study confirming the previously reported antidepressant effect of MOLE (Kou et al. 2018) .

An increased ammonia level in serum was observed in the CCl_4 group, consistent with previous findings (Shal et al. 2020) . Ammonia exists in biological solutions in two forms; NH_3 and NH_4^+. CCl_4-induced liver damage results in hyperammonemia represented by increased levels of circulating ammonia (Damink et al. 2002) . Hyperammonemia is associated with neurological disorders by activating brain oxidative stress and neuroinflammation (Heidari et al. 2016) . Hyperammonemia results from liver injury, and ammonia can easily pass through BBB, causing neurotoxicity (Bosoi and Rose 2009) .

The current study assessed the antiapoptotic effect of MOLE pretreatment against CCl4-induced apoptosis by evaluating the relative caspase 3 mRNA level. A decrease in caspase 3 expression in the presence of MOLE confirms the antidepressant effect of MOLE as suggested by Khan et al. (2019) . Apoptosis can be triggered by an inflammatory response or by ROS generated by CCl_4 (Liu et al. 2018) . It can also be explained by the proapoptotic effect of corticosteroids on the brain regions, especially HC (Kurek et al. 2016) . Consequently, neuroinflammation, oxidative stress, and apoptosis in the brain cells can cause anxiety and depression-like behavior (Khan et al. 2019) . However, our results proved the anxiolytic and anti-depression properties of MOLE.

To further explore the mechanisms behind the neuroprotective effect of MOLE against CCl_4-induced neurotoxicity, the histopathology of CC and HC was assessed using H&E. The thickness of the DG cellular layer in HC region in CCl_4-challenged mice was found to be

markedly thinner than that in the vehicle group. This result agrees with a previous study (Khan et al. 2019) . Neuron degeneration was also manifested in the CC of CCl_4-treated mice in agreement with Shaalan, Radwan, and Saleh (2017) . However, MOLE attenuated these alterations. Histopathological results were consistent with the biochemical findings.

Conclusions

The present study demonstrates the neuroprotective role of MOLE against CCl_4-induced neurotoxicity as indicated by mitigating the neuroinflammation, brain oxidative stress, apoptosis, biochemical alterations, and histopathological changes in HC and CC, and the significant improvement in anxiety and depression-like behavior. This protective effect can be attributed to the antioxidative and anti-inflammatory characteristics of MOLE which prevent the cascade of HE progression. We suggest that TLR4/2-MyD88/NF-κB signaling pathway could be the main target for the ameliorative effect of MOLE.

Abbreviations

ALT: alanine aminotransferase; AST: aspartate aminotransferase; BBB: blood-brain barrier; CCl_3: trichloromethyl; CCl_4: carbon tetrachloride; CC: cerebral cortex; cDNA: complementary DNA; CHCl3: chloroform; CRF: corticotrophin-releasing factor; DG: dentate gyrus; ELISA: enzyme-linked immunosorbent assay; EPA: United States Environmental Protection Agency; FST: forced swimming test; GSH: reduced glutathione; HE: hepatic encephalopathy; HC: hippocampus; H&E: hematoxylin and eosin; HPLC: High-performance liquid chromatography; HPA: hypothalamic-pituitary-adrenal; IL: interleukin; *i.p.*: intraperitoneally; ISHEN: International Society of Hepatic Encephalopathy and Nitrogen Metabolism; LPO: lipid peroxidation; MDA: malondialdehyde; MOLE: *Moringa oleifera* Lam. leaf ethanolic extract; MYD88: myeloid differentiation primary response 88; NF-κB: nuclear factor-kappa B; ROS: reactive oxygen species; RT-qPCR: quantitative reverse transcription-polymerase chain reaction; SOD: superoxide dismutase; TLR: toll-like receptor; TNF: tumor necrosis factor; TST: tail suspension test.

References

Aldridge DR, Tranah EJ, Shawcross DL (2015) Pathogenesis of hepatic encephalopathy: role of ammonia and systemic inflammation. J Clin Exp Hepatol 5:S7-S20

Bancroft JD, Gamble M (2008) Theory and practice of histological techniques. Elsevier health sciences

Bosoi CR, Rose CF (2009) Identifying the direct effects of ammonia on the brain. Metab Brain Dis 24(1):95-102

Bradford MM (1976) A rapid and sensitive method for the quantitation of microgram quantities of protein utilizing the principle of protein-dye binding. Anal Biochem 72(1-2):248-254

Brown J, Wang H, Hajishengallis GN, Martin M (2011) TLR-signaling networks: an integration of adaptor molecules, kinases, and cross-talk. J Dent Res 90(4):417-427

Cristóvão AC, Campos FL, Je G, Esteves M, Guhathakurta S, Yang L, Beal MF, Fonseca BM, Salgado AJ, Queiroz J (2020) Characterization of a Parkinson's disease rat model using an upgraded paraquat exposure paradigm. Eur J Neurosci 52(4):3242-3255

Damink SWMO, Jalan R, Redhead DN, Hayes PC, Deutz NEP, Soeters PB (2002) Interorgan ammonia and amino acid metabolism in metabolically stable patients with cirrhosis and a TIPSS. Hepatology 36(5):1163-1171

Dowlati Y, Herrmann N, Swardfager W, Liu H, Sham L, Reim EK, Lanctôt KL (2010) A meta-analysis of cytokines in major depression. Biol Psychiatry 67(5):446-457

El-Marasy SA, El Awdan SA, Abd-Elsalam RM (2019) Protective role of chrysin on thioacetamide-induced hepatic encephalopathy in rats. Chem Biol Interact 299:111-119

Fakurazi S, Sharifudin SA, Arulselvan P (2012) Moringa oleifera hydroethanolic extracts effectively alleviate acetaminophen-induced hepatotoxicity in experimental rats through their antioxidant nature. Molecules 17(7):8334-8350

Fathy SM, Mahmoud MS (2021) Moringa oleifera Lam. leaf extract mitigates carbon tetrachloride-mediated hepatic inflammation and apoptosis via targeting oxidative stress and toll-like receptor 4/ nuclear factor kappa B pathway in mice. Food Sci. Hum. wellness 10(3):383-391

Fathy S, Said N (2019) Immunomodulation and antigenotoxic effects of propolis in paclitaxel-treated rats. Egypt J Zool 72(72):45-56

Furtado M, Katzman MA (2015) Examining the role of neuroinflammation in major depression. Psychiatry Res 229(1-2):27-36

Gutiérrez-de-Juan V, López de Davalillo S, Fernández-Ramos D, Barbier-Torres L, Zubiete-Franco I, Fernández-Tussy P, Simon J, Lopitz-Otsoa F, de Las Heras J, Iruzubieta P (2017) A morphological method for ammonia detection in liver. PLoS One 12(3):e0173914

Hafkenscheid JC, Dijt CC (1979) Determination of serum aminotransferases: activation by pyridoxal-5'-phosphate in relation to substrate concentration. Clin Chem 25(1):55-59

Han C, Sun T, Xv G, Wang S, Gu J, Liu C (2019) Berberine ameliorates CCl4-induced liver injury in rats through regulation of the Nrf2-Keap1-ARE and p53 signaling pathways. Mol Med Rep 20(4):3095-3102

Heidari R, Jamshidzadeh A, Niknahad H, Mardani E, Ommati MM, Azarpira N, Khodaei F, Zarei A, Ayarzadeh M, Mousavi S (2016) Effect of taurine on chronic and acute liver injury: Focus on blood and brain ammonia. Toxicol reports 3:870-879

Idoga ES, Ambali SF, Ayo JO, Mohammed A (2018) Assessment of antioxidant and neuroprotective activities of methanol extract of Moringa oleifera Lam. leaves in subchronic chlorpyrifos-intoxicated rats.

Comp Clin Path 27(4):917-925

Jollow DJ, Mitchell JR, Zampaglione N al, Gillette JR (1974) Bromobenzene-induced liver necrosis. Protective role of glutathione and evidence for 3, 4-bromobenzene oxide as the hepatotoxic metabolite. Pharmacology 11(3):151-169

Khan A, Shal B, Naveed M, Shah FA, Atiq A, Khan NU, Kim YS, Khan S (2019) Matrine ameliorates anxiety and depression-like behaviour by targeting hyperammonemia-induced neuroinflammation and oxidative stress in CCl4 model of liver injury. Neurotoxicology 72:38-50

Kong Y, Le Y (2011) Toll-like receptors in inflammation of the central nervous system. Int Immunopharmacol 11(10):1407-1414

Kou X, Li B, Olayanju JB, Drake JM, Chen N (2018) Nutraceutical or pharmacological potential of Moringa oleifera Lam. Nutrients 10(3):343

Kubera M, Obuchowicz E, Goehler L, Brzeszcz J, Maes M (2011) In animal models, psychosocial stress-induced (neuro) inflammation, apoptosis and reduced neurogenesis are associated to the onset of depression. Prog Neuro-Psychopharmacology Biol Psychiatry 35(3):744-759

Kurek A, Kucharczyk M, Detka J, Ślusarczyk J, Trojan E, Głombik K, Bojarski B, Ludwikowska A, Lasoń W, Budziszewska B (2016) Pro-apoptotic action of corticosterone in hippocampal organotypic cultures. Neurotox Res 30(2):225-238

Liu Y, Wen P, Zhang X, Dai Y, He Q (2018) Breviscapine ameliorates CCl4-induced liver injury in mice through inhibiting inflammatory apoptotic response and ROS generation. Int J Mol Med 42(2):755-768

Lıu Z, Tıan J (2016) Changes of MDA and SOD in brain tissue after secondary brain injury with seawater immersion in rats. Turk Neurosurg 26(3):384-388

Lu L, Wu C, Lu B, Xie D, Wang Z, Azami NLB, An Y, Wang H, Ye G, Sun M (2020) BabaoDan cures hepatic encephalopathy by decreasing ammonia levels and alleviating inflammation in rats. J Ethnopharmacol 249:112301

Mahdi HJ, Khan NAK, Asmawi MZ Bin, Mahmud R, Vikneswaran A, Murugaiyah L (2018) In vivo anti-arthritic and anti-nociceptive effects of ethanol extract of Moringa oleifera leaves on complete Freund's adjuvant (CFA)-induced arthritis in rats. Integr Med Res 7(1):85-94

Makni M, Chtourou Y, Barkallah M, Fetoui H (2012) Protective effect of vanillin against carbon tetrachloride (CCl4)-induced oxidative brain injury in rats. Toxicol Ind Health 28(7):655-662

Mao S-S, Hua R, Zhao X-P, Qin X, Sun Z-Q, Zhang Y, Wu Y-Q, Jia M-X, Cao J-L, Zhang Y-M (2012) Exogenous administration of PACAP alleviates traumatic brain injury in rats through a mechanism involving the TLR4/MyD88/NF-κB pathway. J Neurotrauma 29(10):1941-1959

Mello BSF, Monte AS, McIntyre RS, Soczynska JK, Custódio CS, Cordeiro RC, Chaves JH, Vasconcelos SMM, Júnior HVN, de Sousa FCF (2013) Effects of doxycycline on depressive-like behavior in mice after lipopolysaccharide (LPS) administration. J Psychiatr Res 47(10):1521-1529

Millan MJ (2004) The role of monoamines in the actions of established and “novel” antidepressant agents: a critical review. Eur J Pharmacol 500(1-3):371-384

Nunes-Souza V, Alenina N, Qadri F, Penninger JM, Santos RAS, Bader M, Rabelo LA (2016) CD36/sirtuin 1 axis impairment contributes to hepatic steatosis in ACE2-deficient mice. Oxid. Med. Cell. Longev. 2016:

Ogaly HA, Eltablawy NA, Abd-Elsalam RM (2018) Antifibrogenic influence of Mentha piperita L. essential oil against CCl4-induced liver fibrosis in rats. Oxid. Med. Cell. Longev. 2018:

Ohkawa H, Ohishi N, Yagi K (1979) Assay for lipid peroxides in animal tissues by thiobarbituric acid reaction. Anal Biochem 95(2):351-358

Porsolt RD, Bertin A, Jalfre M (1977) Behavioral despair in mice: a primary screening test for antidepressants. Arch Int Pharmacodyn Ther 229(2):327

Risal P, Hwang PH, Yun BS, Yi H-K, Cho BH, Jang KY, Jeong YJ (2012) Hispidin analogue davallialactone attenuates carbon tetrachloride-induced hepatotoxicity in mice. J Nat Prod 75(10):1683-1689

Sampson EJ, Whitner VS, Burtis CA, McKneally SS, Fast DM, Bayse DD (1980) An interlaboratory evaluation of the IFCC method for aspartate aminotransferase with use of purified enzyme materials. Clin Chem 26(8):1156-1164

Shaalan S, Radwan OK, Saleh H (2017) Role of Wheat Germ Oil against Carbon Tetrachloride Induced Neurotoxicity in Brain Tissues of Adult Male Mice. Egypt J Zool 174(5542):1-18

Shal B, Khan A, Naveed M, Ali H, Seo EK, Choi H, Khan S (2020) Neuroprotective effect of 25-Methoxyhispidol A against CCl4-induced behavioral alterations by targeting VEGF/BDNF and caspase-3 in mice. Life Sci 117684

Shim J-Y, Kim M-H, Kim H-D, Ahn J-Y, Yun Y-S, Song J-Y (2010) Protective action of the immunomodulator ginsan against carbon tetrachloride-induced liver injury via control of oxidative stress and the inflammatory response. Toxicol Appl Pharmacol 242(3):318-325

Singh D, Arya PV, Aggarwal VP, Gupta RS (2014) Evaluation of antioxidant and hepatoprotective activities of Moringa oleifera Lam. leaves in carbon tetrachloride-intoxicated rats. Antioxidants 3(3):569-591

de Souza Machado F, Marinho JP, Abujamra AL, Dani C, Quincozes-Santos A, Funchal C (2015) Carbon tetrachloride increases the pro-inflammatory cytokines levels in different brain areas of Wistar rats: the protective effect of acai frozen pulp. Neurochem Res 40(9):1976-1983

Steru L, Chermat R, Thierry B, Simon P (1985) The tail suspension test: a new method for screening antidepressants in mice. Psychopharmacology (Berl) 85(3):367-370

Tesfay SZ, Bertling I, Odindo AO, Workneh TS, Mathaba N (2011) Levels of anti-oxidants in different parts of moringa (Moringa oleifera) seedling. African J Agric Res 6(22):5123-5132

Vairappan B, Sundhar M, Srinivas BH (2019) Resveratrol Restores Neuronal Tight Junction Proteins Through Correction of Ammonia and Inflammation in CCl 4-Induced Cirrhotic Mice. Mol Neurobiol 56(7):4718-4729

Valentine JS, Hart PJ (2003) Misfolded CuZnSOD and amyotrophic lateral sclerosis. Proc Natl Acad Sci 100(7):3617-3622

Vogelzangs N, Beekman ATF, De Jonge P, Penninx B (2013) Anxiety disorders and inflammation in a large adult cohort. Transl Psychiatry 3(4):e249-e249

Yoshimura A, Shichita T (2012) Post-ischemic inflammation in the brain. Front Immunol 3:132

Yue S, Xue N, Li H, Huang B, Chen Z, Wang X (2020) Hepatoprotective Effect of Apigenin Against Liver Injury via the Non-canonical NF-κB Pathway In Vivo and In Vitro. Inflammation

Zhou Z, Hou J, Mo Y, Ren M, Yang G, Qu Z, Hu Y (2020) Geniposidic acid ameliorates spatial learning and memory deficits and alleviates neuroinflammation via inhibiting HMGB-1 and downregulating TLR4/2 signaling pathway in APP/PS1 mice. Eur J Pharmacol 869:172857

Declarations

Ethical Approval

Animal experimentation protocols were carried out following the National Institutes of Health (NIH) guidelines for animal experimentation and approved by Cairo University Institutional Animal Care and Use Committee (CU-IACUC), Egypt, (permission number: CU/I/F/41/20).

Consent to Participate

Not applicable.

Consent to Publish

Not applicable.

Authors' contributions

All authors designed the experimental protocol, were involved in the implementation of the overall study, performed the statistical analyses of the study, wrote the manuscript, and contributed to the critical revision of the manuscript.

Availability of data and materials

The authors declare that the datasets used and/or analysed during the current study are available from the corresponding author on reasonable request.

Conflict of interest

There are no conflicts of interest to declare.

Funding

The authors are grateful to the Deanship of Scientific Research at King Khalid University in Saudi Arabia for financing this work under the research group program, award number (R.G.P. 2/31/40).

Tables

Table 1: Primer sequences used for RT-qPCR

Genes	Forward primer (5′-3′)	Reverse primer (5′-3′)	Reference
TLR2	5′ CAAATGGATCATTGACAACATCATC 3′	5′ TTCGTACTTGCACCACTCGC 3′	(Peng et al. 2015)
TLR4	5′ GCTTGAATCCCTGCATAGAGGTAG 3′	5′ TCTTCAAGGGGTTGAAGCTCAG 3′	(S. M. Fathy and Mahmoud 2021)
MYD88	5′ GGAACAGACCAACTATCGGC 3′	5′ GAGACAACCACTACCATCCG 3′	(Wang et al. 2017)
NF-κB	5′ AAGGATGTCTCCACACCACTG 3′	5′ CACTGTCTGCCTCTCTCGTCT 3′	(S. M. Fathy and Mahmoud 2021)
Caspase 3	5′ CCTCAGAGAGACATTCATGG 3′	5′ GCAGTAGTCGCCTCTGAAGA 3′	(Zhang et al. 2019)
GAPDH	5′ CATCAACGGGAAGCCCATC 3′	5′ CTCGTGGTTCACACCCATC 3′	(S. M. Fathy and Mahmoud 2021)

Table 2. MOLE pretreatment effect on the relative expression of *TLR2, TLR4, MyD88, NF-κB,* and *caspase 3* as well as the protein levels of TNF-α and IL6 in the hippocampus (HC) and cerebral cortex (CC) of CCl_4-injected mice.

			Vehicle	CCl_4	MOLE	CCl_4+MOLE
Relative mRNA expression (fold change over vehicle)	*TLR2*	HC	1.01 ± 0.007071	5.000 ± 0.1414 ***	1.090 ± 007071	2.100 ± 0.4950 ##
		CC	1.01 ± 0.007071	6.000 ± 0.1414 ***	0.9800 ± 007071	2.800 ± 0.4950 ###
	TLR4	HC	1.030 ± 0.01414	7.000 ± 0.4243 ***	1.010 ± 0.02121	3.500 ± 0.3465 ###
		CC	1.010 ± 0.01414	7.000 ± 0.4243 ***	1.020 ± 0.02121	3.010 ± 0.3465 ###
	MyD88	HC	1.010 ± 0.03512	5.000 ± 0.07071 ****	1.020 ± 0.01414	1.900 ± 0.1131 ####
		CC	1.000 ± 0.02121	5.000 ± 0.07071 ****	1.000 ± 0.01414	2.060 ± 0.1131 ####
	NF-κB	HC	1.080 ± 0.03512	10.00 ± 1.701 **	1.010 ± 007071	4.010 ± 0.4050 ##
		CC	1.010 ± 0.03512	6.000 ± 1.701 *	1.050 ± 007071	3.200 ± 0.4050
	Caspase 3	HC	1.000 ± 0.02121	6.000 ± 0.2121 ****	1.100 ± 0.01414	2.900 ± 0.1414 ####
		CC	1.030 ± 0.02121	6.000 ± 0.2121 ****	1.200 ± 0.02121	2.700 ± 0.1414 ####
Protein level (pg/mg)	TNF-α	HC	28.60 ± 3.606	118.0 ± 6.010 **	26.50 ± 6.000	68.40 ± 18.03 #
		CC	33.70 ± 3.606	126.0 ± 6.010 **	35.10 ± 6.000	42.90 ± 18.03 ##
	IL-6	HC	52.10 ± 8.910	141.0 ± 18.17 **	36.10 ± 1.000	82.30 ± 12.59 #
		CC	39.50 ± 8.910	167.0 ± 18.17 **	38.40 ± 1.000	64.50 ± 12.59 ##

TLR: toll-like receptor, *MYD88*: myeloid differentiation primary response 88, *NF-κB*: nuclear factor kappa B, TNF-α: tumor necrosis factor- α, IL-6: interleukin 6. All data are represented as mean ± SD, n=8. *: $P < 0.05$, **: $P < 0.01$, ***: $P < 0.001$, and ****: $P < 0.0001$ compared to vehicle group. #: $P < 0.05$, ##: $P < 0.01$, ###: $P < 0.001$, and ####: $P < 0.0001$ compared to CCl_4 group.

Figures

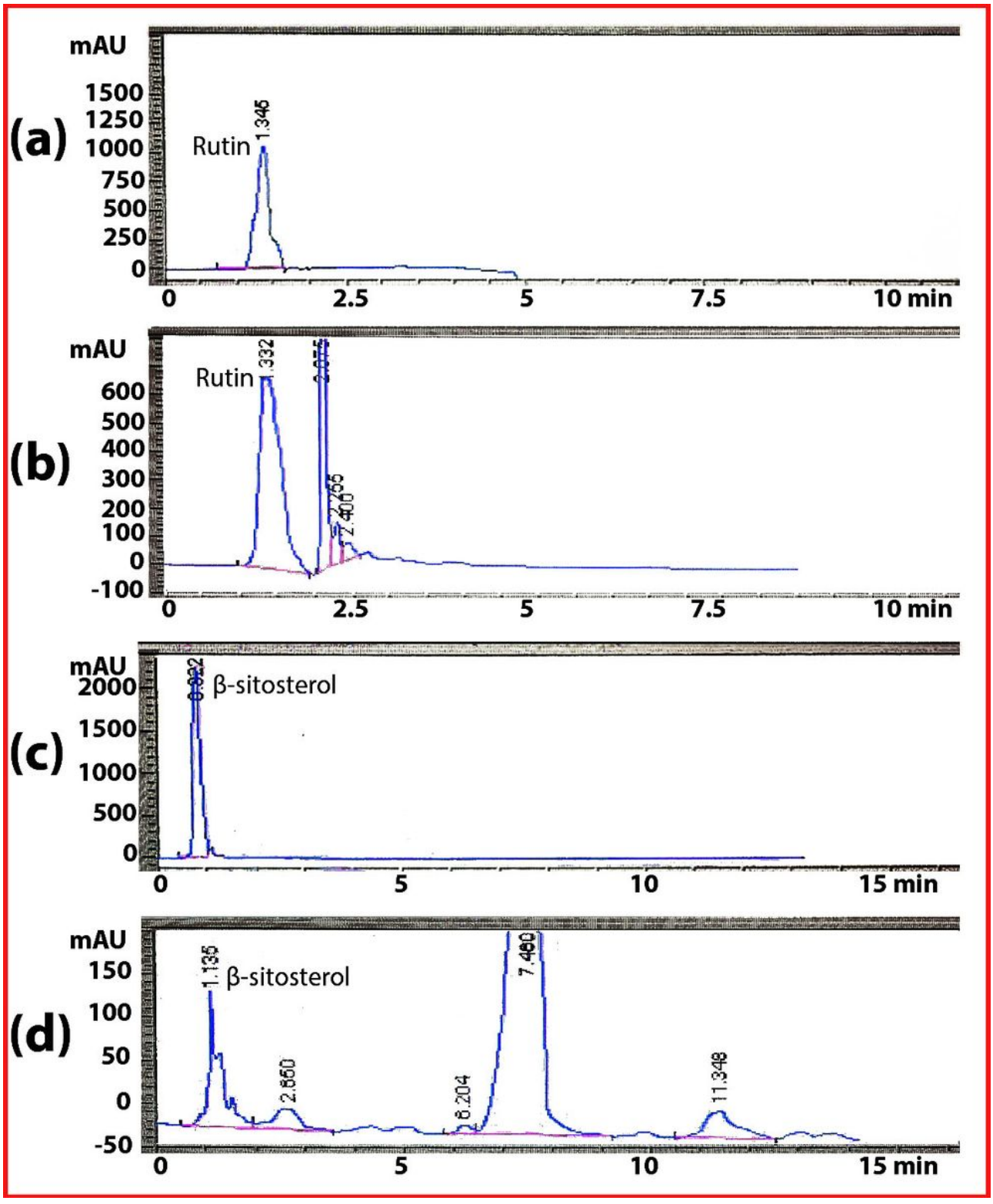

Figure 1

HPLC chromatograms (λ 254 nm) of **(a)** rutin reference standard (retention time 1.3 min), and **(b)** leaf ethanolic extract of MOL; HPLC chromatograms (λ 210 nm) of **(c)** β-sitosterol reference standard (retention time 0.8 min), and **(d)** leaf ethanolic extract of MOL.

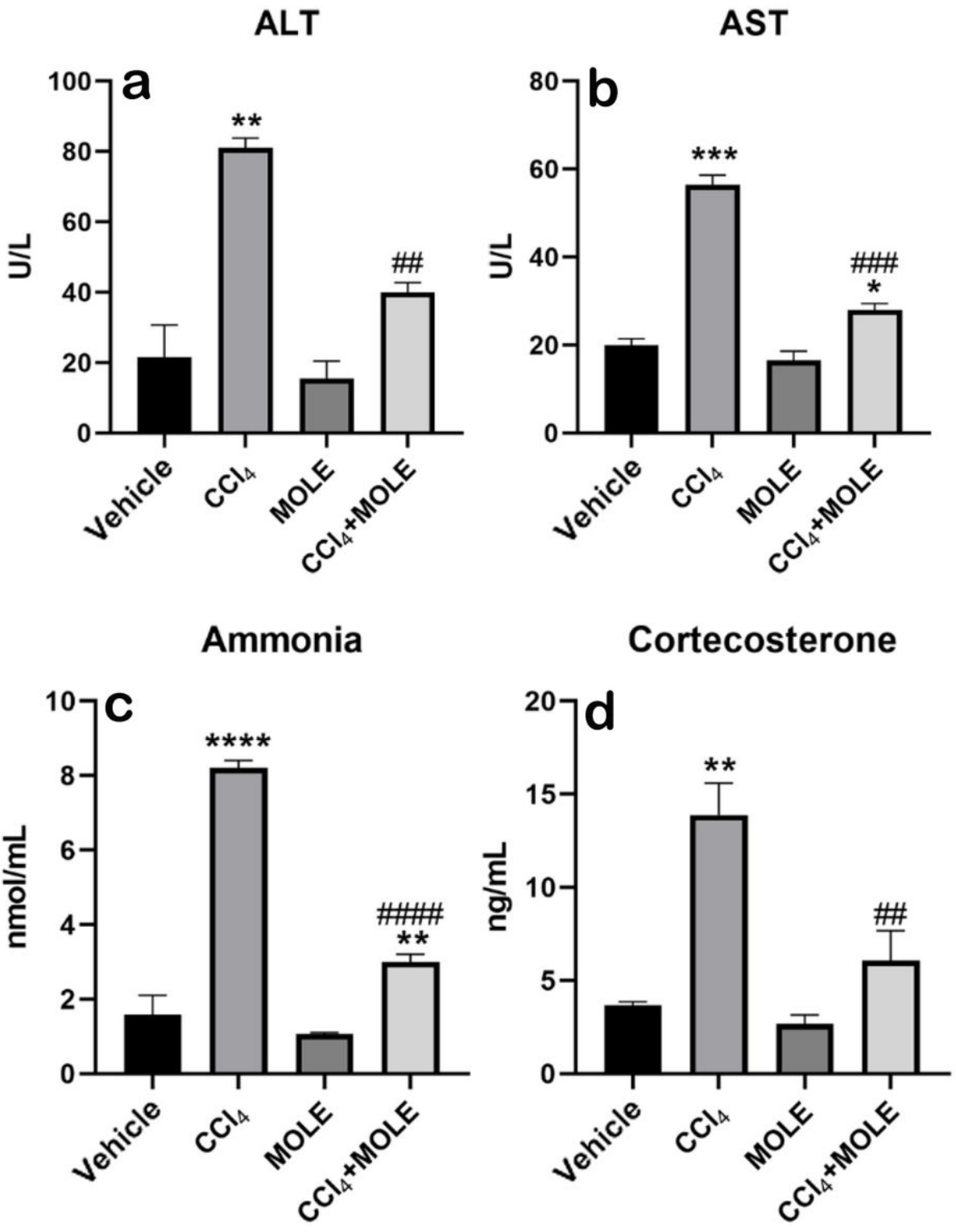

Figure 2

Protective effect of MOLE pretreatment on serum aminotransferases, ammonia and corticosterone levels. MOLE pretreatment protects against the increase in the levels of alanine aminotransferase (ALT) **(a)**, aspartate aminotransferase (AST) **(b)**, ammonia **(c)**, and corticosterone **(d)** induced by CCl_4. All data are represented as mean ± SD, n=8. *: $P < 0.05$, **: $P < 0.01$, ***: $P < 0.001$, and ****: $P < 0.0001$ compared to vehicle group. ##: $P < 0.01$, ###: $P < 0.001$, and ####: $P < 0.0001$ compared to CCl_4 group.

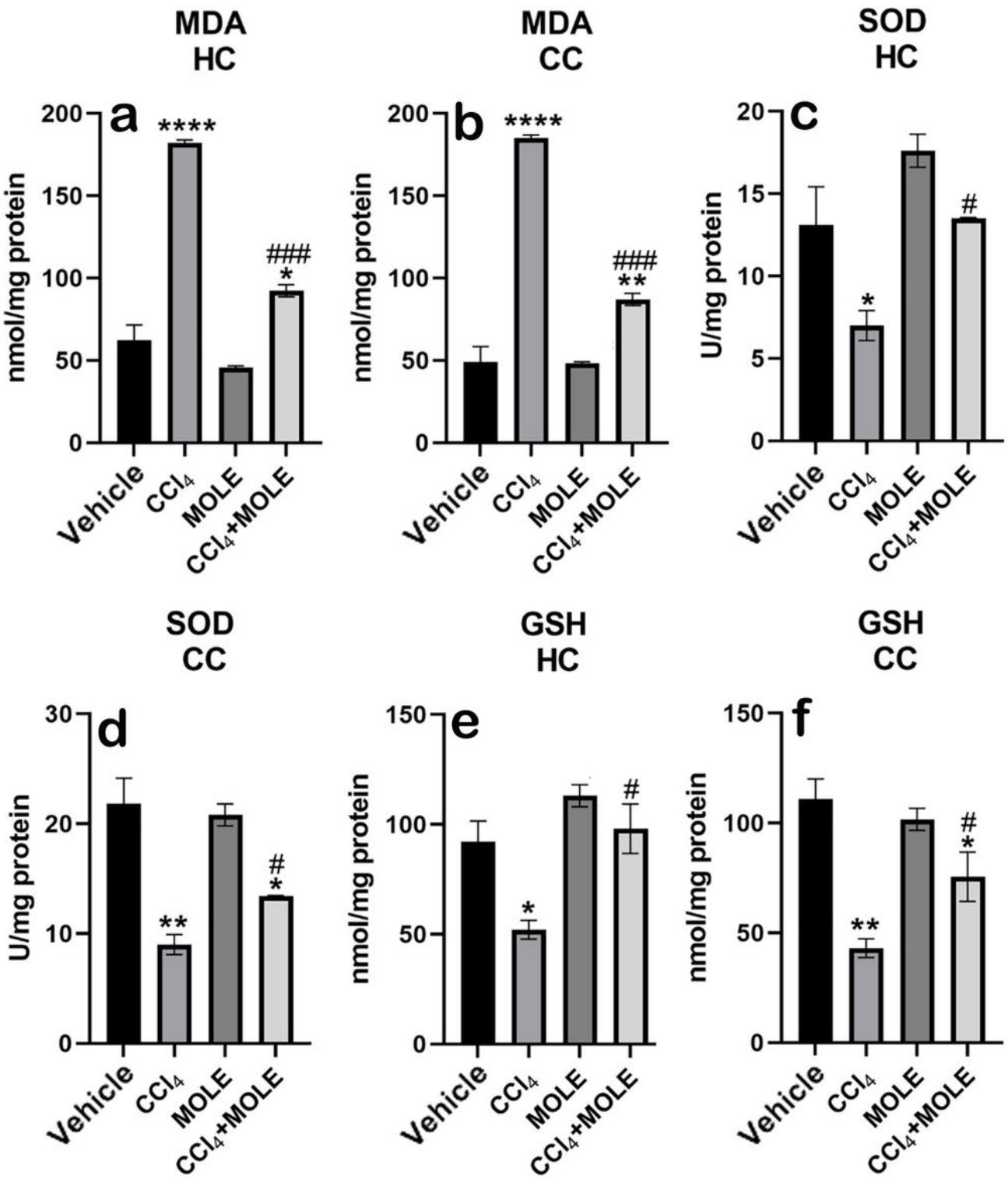

Figure 3

MOLE pretreatment impact on lipid peroxidation (LPO) and antioxidant mechanisms in the hippocampus (HC) and cerebral cortex (CC). MOLE pretreatment attenuates elevated LPO, represented by malondialdehyde (MDA), by CCl_4 toxicity in the HC **(a)** and CC **(b)**. It also restores antioxidant mechanisms, represented by superoxide dismutase (SOD) in the HC **(c)** and CC **(d)** and reduced glutathione (GSH) elevated by CCl_4 toxicity in the HC **(e)** and CC **(f)**. All data are represented as mean ±

SD, n=8. *: $P < 0.05$, **: $P < 0.01$, and ****: $P < 0.0001$ compared to vehicle group. #: $P < 0.05$, ###: $P < 0.001$, and ####: $P < 0.0001$ compared to CCl_4 group.

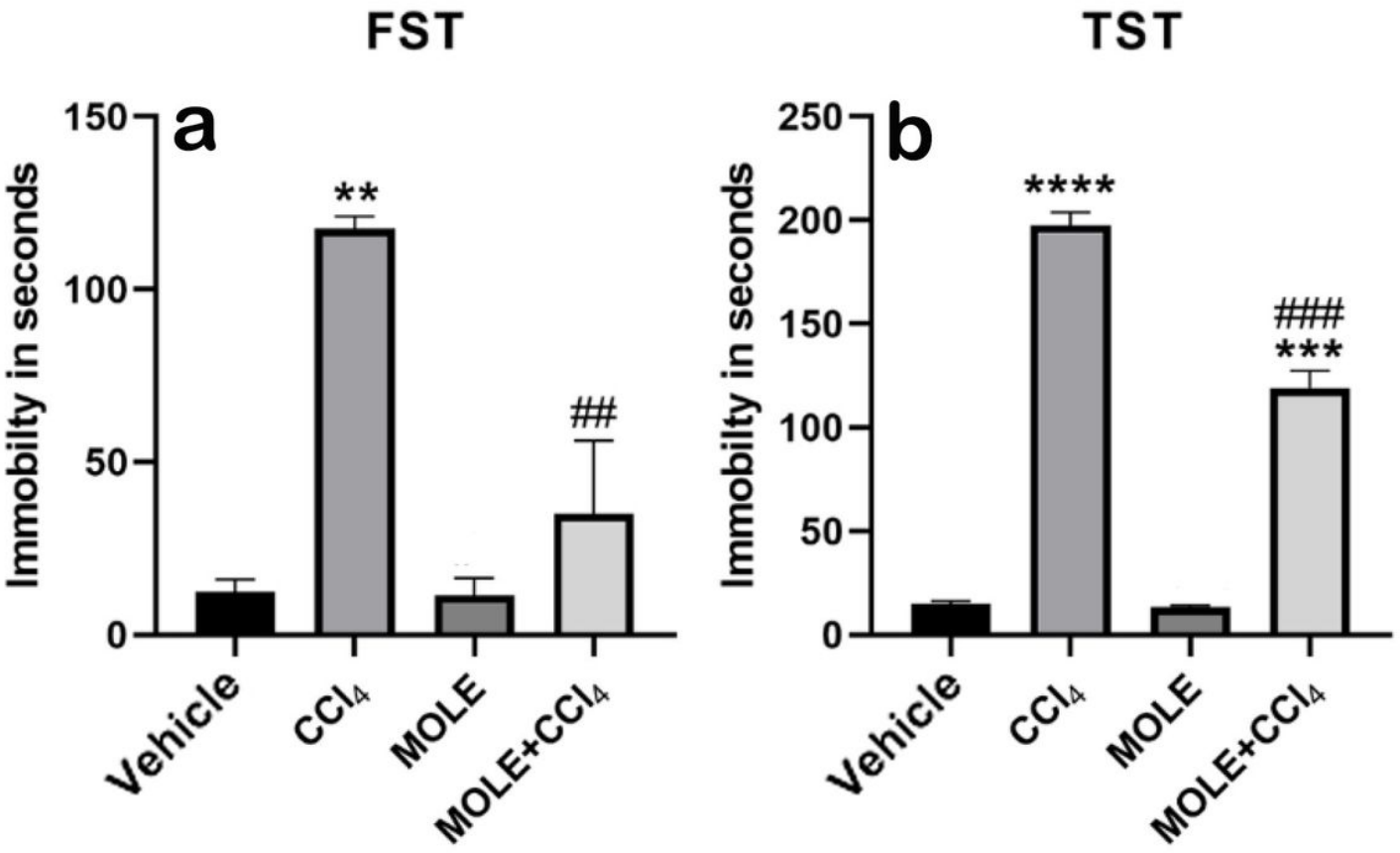

Figure 4

MOLE pretreatment influence on the depression-like behaviors induced by CCl_4. MOLE pretreatment protects against the exhibition of depression-like behaviors induced by CCl_4 based on forced swimming test (FST) **(a)** and tail suspension test (TST) **(b)**. All data are represented as mean ± SD, n=8. **: $P < 0.01$, ***: $P < 0.001$, and ****: $P < 0.0001$ compared to vehicle group. ##: $P < 0.01$, and ###: $P < 0.001$ compared to CCl_4 group.

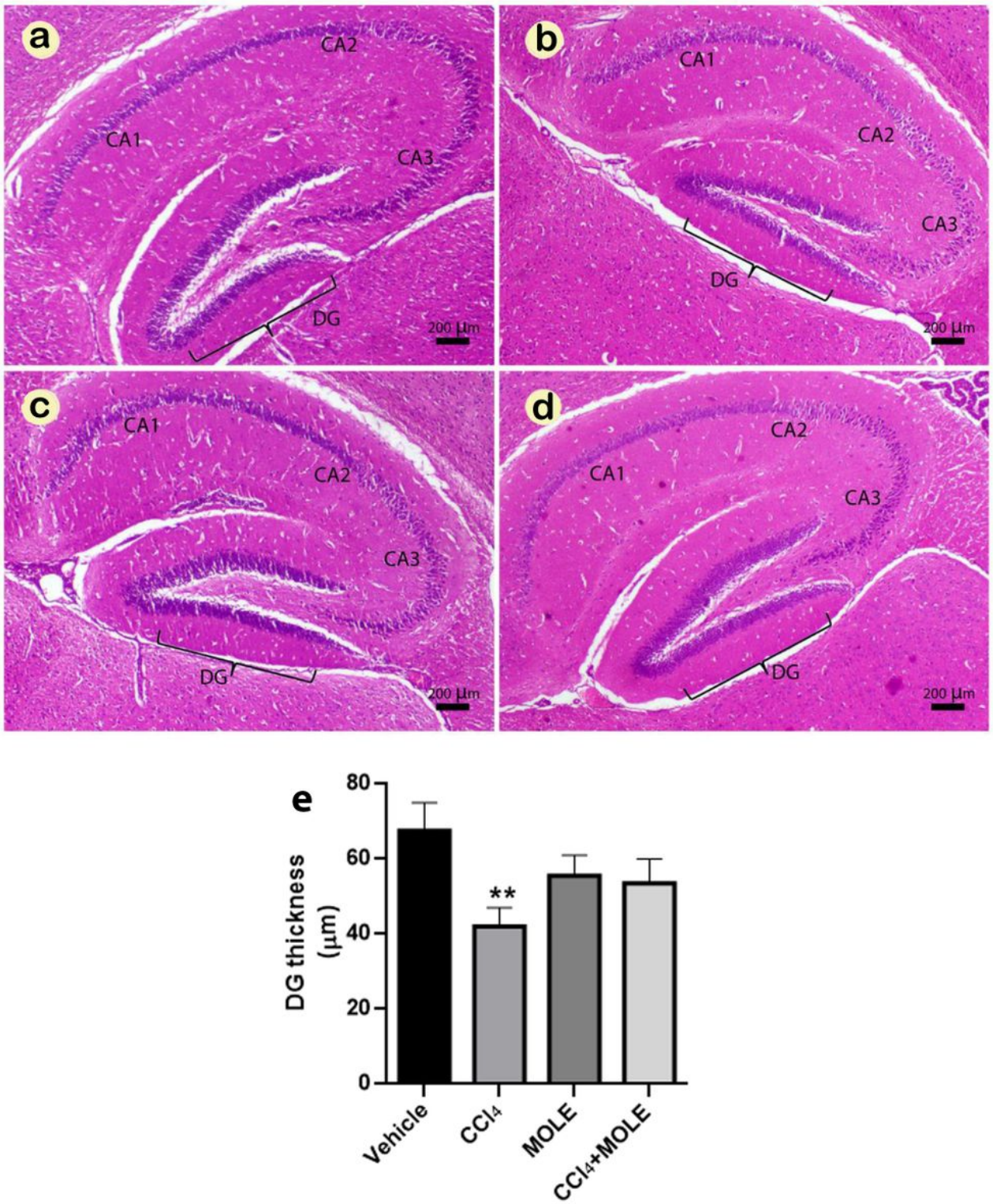

Figure 5

MOLE pretreatment effect on the induced histopathological changes in the hippocampus (HC) by CCl_4 administration. Micrographs **(a, b, c and d)** show coronal sections in the HC stained with H&E (40x magnification, scale bar=200µm) of vehicle, CCl_4, MOLE, and CCl_4+MOLE groups, respectively. CA1, CA2, and CA3 denote different regions of cornu ammonis (CA). DG denotes dentate gyrus. Graph **(e)** shows

that MOLE pretreatment protects against the reduction in DG thickness induced by CCl_4. All data are represented as mean ± SD, n=8. **: $P < 0.01$ compared to vehicle group.

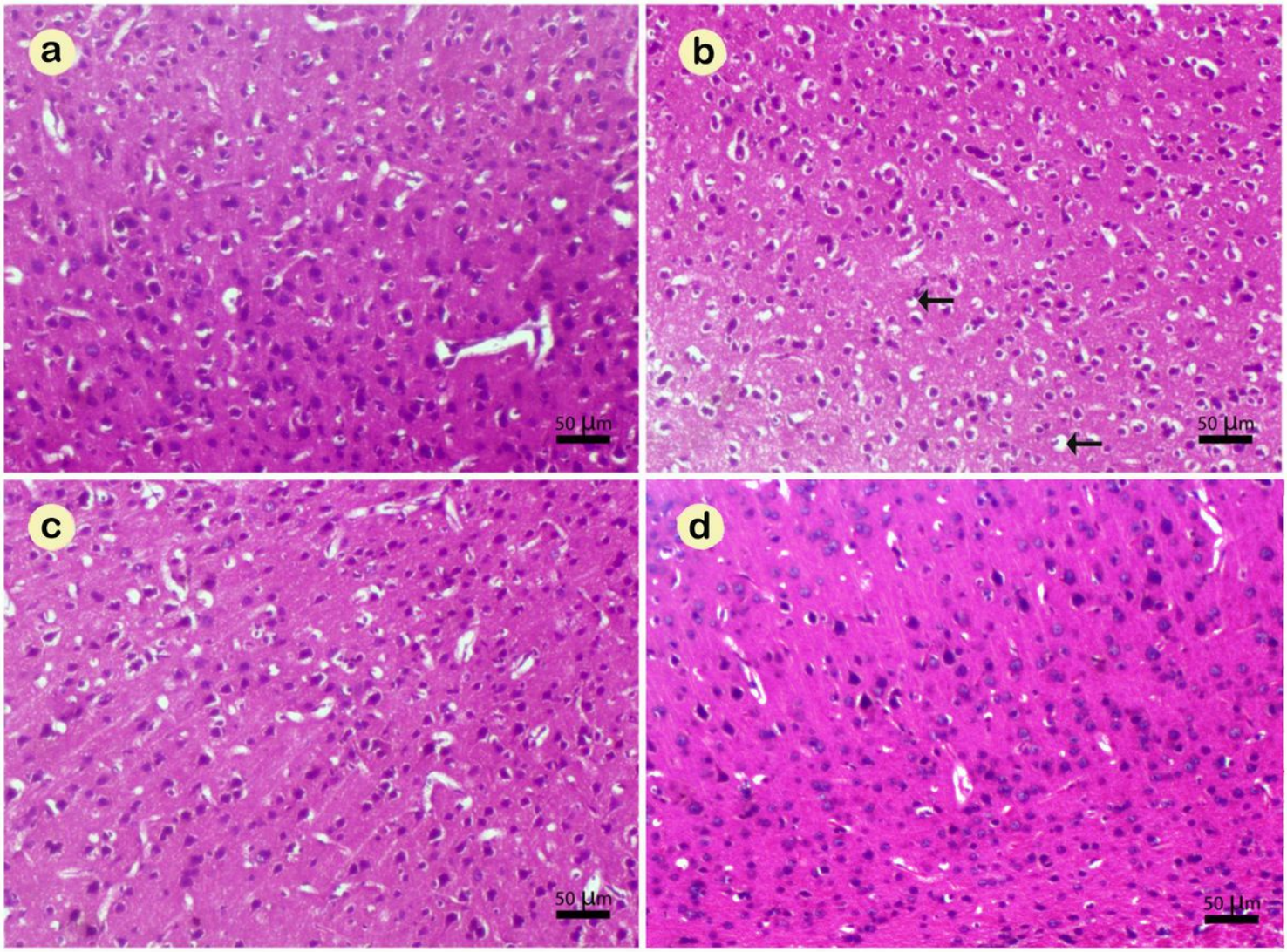

Figure 6

MOLE pretreatment effect on the induced histopathological changes in the cerebral cortex (CC) by CCl_4 administration.

Micrographs **(a, b, c and d)** show coronal sections in the CC (100x magnification, scale bar=50µm) of vehicle, CCl_4, MOLE, and CCl_4+MOLE groups, respectively. Neuron degeneration is manifested in the CCl_4 group but MOLE pretreatment protected the neurons against this effect.